








RESEARCH ARTICLE

WILEY

A fuzzy control system for energy-efficient wireless devices in the Internet of vehicles

Mario Collotta¹  | Renato Ferrero²  | Edoardo Giusto²  |
Mohammad Ghazi Vakili²  | Jacopo Grecuccio²  |
Xiangjie Kong³  | Ilsun You⁴ 

¹Computer Engineering and Networks Laboratory, Faculty of Engineering and Architecture, Università degli Studi di Enna, Kore, Enna, Italy

²Dipartimento di Automatica e Informatica, Politecnico di Torino, Turin, Italy

³College of Computer Science and Technology, Zhejiang University of Technology, Hangzhou, China

⁴Department of Information Security Engineering, Soonchunhyang University, Asan-si, Choongchungnam-do, Korea

Correspondence

Ilsun You, Department of Information Security Engineering, Soonchunhyang University, Asan-si, Choongchungnam-do 31538, Korea.
Email: ilsunu@gmail.com

Funding information

The Soonchunhyang University Research Fund

Abstract

Embedded systems are common in the Internet of Things domain: their integration in vehicles and mobile devices is being fostered in the Internet of vehicles (IoV). IoV has direct applications on intelligent transportation systems and smart cities. Besides basic requirements, such as ease of installation, cost-effectiveness, scalability, and flexibility, IOV applications need to guarantee energy-efficient and good-quality communication. In fact, IoV implementations are commonly based on wireless nodes, which rely on a limited energy source; therefore, an efficient communication among the nodes is desirable to prolong the lifetime of the devices. In particular, the alternation of active and sleep states and the regulation of the transmission power represent two common approaches to save energy. Based on this strategy, an effective fuzzy control system is presented in the paper to manage power consumption and quality of services of IoV applications. Two fuzzy controllers increase the battery life while keeping a good throughput to workload ratio. This technique has been simulated with two leading technologies in IoV: IEEE 802.11b/g/n and IEEE 802.11p. Experimental results show a network lifetime improvement ranging from 30% to 40%, according to the adopted medium access control protocol.

KEYWORDS

fuzzy logic, intervehicle communication, power consumption, power savings, quality of service

1 | INTRODUCTION

The technological equipment of vehicles is continuously advancing to make the driving experience safer and more pleasant. Radar and front camera can track the car ahead for adaptive cruise control¹ and automatic emergency braking,² ultrasonic sensors can recognize the parking spot for automatic parking assist,³ services exploiting positioning systems such as global positioning system (GPS) and Galileo give directions and suggest alternate routes during navigation,⁴ and so forth. A driver directly enjoys the benefits of the data collected and processed by his or her vehicle, but more advantages, both for the driver and the whole community, can be obtained by sharing the collected information among the vehicles. In fact, intervehicle communication is often regarded as a basic requirement for developing intelligent transportation systems⁵ and, more in general, for designing smart cities.⁶

The possibility of transmitting information among vehicles has been exploited for 20 years in building vehicular ad-hoc networks (VANETs).⁷ A VANET is a kind of mobile wireless network, which is spontaneously created when vehicles establish a wireless communication among themselves or with roadside units (RSUs), such as traffic lights and traffic signs. Research in this field has shown useful applications of VANETs—for example, traffic management,⁸ emergency notification,⁹ sustainable mobility¹⁰—but it has also pointed out some critical issues. First, the topology of a VANET is highly dynamic due to the different speed and route of vehicles. As new vehicles continuously join the network whereas others move outside the coverage area, participation in the VANET is temporary and unpredictable, with a local range of usage. Second, VANETs behave as a close environment: communication with personal devices to provide a seamless user experience, Internet connectivity to guarantee reliable services, and use of cloud computing and storing to improve performance are not supported in general. The difficulty in providing a global service and networking constraints limit the commercial implementation of VANETs, therefore a more powerful and heterogeneous paradigm is emerging: the Internet of vehicles (IoV).^{11–13}

Two main advancements can be recognized in the vision of IoV with respect to traditional VANETs. First, the intervehicle communication in VANETs basically consists of vehicle-to-vehicle and vehicle-to-roadside communication.¹⁴ Instead, the IoV network is more heterogeneous and aims at integrating vehicles with humans, intelligent devices, environment, and other networks.¹⁵ As a consequence, besides vehicle-to-vehicle and vehicle-to-roadside, other kinds of communication are supported: vehicle-to-pedestrian, vehicle-to-personal devices, vehicle-to-sensors, vehicle-to-infrastructure.¹¹ Second, IoV services are intended for big communities, like a metropolitan area, and the large amount of data demands proper computing and reasoning capabilities. Thus, the data collected by a vehicle usually are not processed internally: storage, processing, and analysis are delegated to a cloud infrastructure.¹² Heterogeneity and use of cloud computing require some considerations in the design of IoV.

The heterogeneity of IoV implies a large variety of kinds of information exchanged, ranging from raw data collected by sensors—such as speed for traffic light management¹⁶—to large size content, such as video streaming for increasing the visual range of following vehicles,¹⁷ and in

general any kind of media file shared for infotainment.¹⁸ The variety of connected entities, exchanged content, and implemented applications with different purposes and requirements has led to the definition of several medium access control (MAC) protocols for IoV. In particular, IEEE 802.11p, also known as wireless access in vehicular environments (WAVE), enhances the IEEE 802.11 standard (Wi-Fi) for IoV: for example, it relaxes the authentication procedure, as mobility shortens the communication time, and adds timing advertisement for the synchronization with a common time reference.¹⁹ The dedicated short-range communications (DSRC) standard, in the United States,²⁰ and the ETSI ITS-G5, in Europe,²¹ are both based on IEEE 802.11p for enabling high-speed and secure intervehicle communication. The corresponding standard adopted in Japan is T109,²² which is defined by the Association of Radio Industries and Businesses (ARIB). Besides these standards, several other MAC protocols have been proposed in the scientific literature for the wireless communication in IoV.

Relying on cloud services for information storage and management increases the size of data transmitted by every device in the IoV network. Depending on the network architecture, the traffic size can be remarkable for bridge nodes, that is, nodes that collect information from leaf nodes and forward it toward a sink node. The volume of traffic impacts directly on energy consumption, as elaboration and transmission of the collected data are high power-demanding activities.²³ Energy consumption is particularly critical when the devices are battery-supplied.²⁴ The paper addresses this issue by proposing a mechanism based on two fuzzy logic controllers (FLCs) for energy-efficient communication. Fuzzy logic is commonly exploited in decision making^{25–27} and optimization techniques,^{28,29} as it can deal with fuzzy information. In the proposed mechanism, fuzzy rules are established to optimize the power consumption without detriment to quality of service (QoS). In the literature, there are several MAC protocols proposed for energy-efficient communication in the IoV scenario. As these protocols are not compliant to any standard, their application in a real scenario is limited. An advantage of the approach proposed in this paper is that it works at high-level, so it can be adopted by standard MAC protocols for IoV.

The main contributions of the paper are:

- a meticulous analysis of the IoV scenario, with the identification of main issues and desiderata;
- a theoretical model of the battery consumption of a wireless node in an IoV application, depending on the operational duty cycle and transmission power;
- the proposal of two distinct fuzzy controllers for extending the node lifetime, based on the theoretical model of the battery consumption;
- a rigorous methodology to design and optimize the fuzzy system according to the identified desiderata;
- a reliable evaluation of the proposed approach following specifications of a real node and standardized MAC protocols for IoV.

The remainder of the paper is organized as follows. Standards and state-of-the-art MAC protocols are reviewed in Section 2, with particular attention to QoS and power savings issues. Section 3 describes the considered scenario and identifies the goals precisely, by defining energy efficiency and QoS. Section 4 explains the proposed solution. The proposed approach is first configured and then evaluated by means of simulations: the simulated scenario is described in Section 5, the configuration procedure is explained in Section 6, and then the performance is evaluated in Section 7. Finally, some conclusions are drawn in Section 8.

2 | RELATED WORK

As information shared in vehicular networks become increasingly heterogeneous, there is the need to find standards and protocols able to manage different types of applications with various requirements. In particular, the network architecture of ITSs should provide a MAC layer able to handle several issues, taking into account the different types of messages. Some of the challenges for the MAC layer in IoV are related to the management of prioritized accesses and the unpredictability of responses. Moreover, providing a reliable broadcast communication in such networks can be difficult due to hidden terminal and exposed node problems. Another important issue is represented by continuous changes of the network topology caused by vehicles traveling at a high velocity. Thus, a MAC protocol should be able to rapidly tackle these changes. Finally, for safety applications, there is the need to ensure very short medium access delays.³⁰

The IEEE 802.11p amendment, derived from IEEE 802.11 standard, has been specifically defined for vehicular networks. Changing the beacon generation rate in this protocol has been frequently investigated for improving the QoS in IoV networks.^{31–35} For example, the beacon messages frequency is tuned to improve network scalability,³¹ and beacon rate is adapted for balancing information accuracy and bandwidth consumption.³²

Besides QoS related issue, power consumption and battery-lifetime are crucial for wireless nodes in IoV networks. When devices have strict requirements for both QoS of transmission and battery lifetime, the MAC layer plays a central role: a correct design and optimizations at this level can help reducing the amount of power that is required for handling data transmission. A fuzzy logic solution is adopted for adaptive optimization. Both contention window size and transmission power can be optimized by means of a fuzzy logic solution that evaluates three parameters: *collision rate*, *Signal-to-Interference-plus-Noise-Ratio (SINR)*, and *queue overflow*.³⁶ The queue overflow represents the packet drop at various stages of transmission. Simulation results show that the proposed fuzzy logic based scheme brought an improved throughput, lower end-to-end delay, and high packet success rate with respect to IEEE 802.11p default existing scheme.

An adaptive transmission power scheme has been proposed to improve QoS in vehicles networks.³⁷ In detail, a multiobjective algorithm takes as input vehicles density and transmission range for estimating the Average-Connected-Coverage. Then, the same values for transmission range and vehicle density are used for running another algorithm which adapts transmission power according to such inputs. Results showed that the adaptive transmission power scheme improves latency, retransmission and throughput of the system with respect to fixed transmission power schemes.

Besides 802.11p, other MAC protocols have been proposed for the IoV scenario, mainly based on a TDMA scheme, such as VeMAC, STDMA, VC-MAC, and DMMAC.^{38–41}

VeMAC assigns disjoint sets of time slots to vehicles moving in opposite direction and to RSUs.³⁸ In the proposed scheme, nodes acquire a time slot by listening the control channel. The frame received through this channel includes the set of one-hop neighbors with their correspondent assigned slots. In this way, each node is aware of the slots used by its neighbors and so it can randomly choose an available slot for transmission. Following this approach, the hidden terminal problem is eliminated and in addition every transmission can be implicitly acknowledged by listening to the following one. This mechanism provides a reliable broadcast.

STDMA follows an attractive approach for periodic traffic, by adopting a reservation scheme consisting of four phases³⁹:

- *Initialization*: After start-up, a node listens to the channel for a complete frame and, once received, determines the allocation status of current slots.

- *Network entry*: The node performs a random access to announce its presence and its first slot reservation.
- *First frame*: The node uses the obtained slot for announcing further slots reservations and their respective duration.
- *Continuous operations*: The node transmits using the previously reserved slots.

The vehicular-cooperative MAC (VC-MAC) protocol addresses the high demand of broadcast data that vehicles have to download from gateways of IoV networks.⁴⁰ It exploits concurrently the concept of cooperative communication and spacial re-usability under broadcast scenarios. The basic idea is allowing “good users” (those having a good channel condition) to act as relay nodes and forward the broadcast messages sent by gateways. Nodes authorized to relay broadcast messages are selected to minimize collisions and maximizing the spacial re-usability. Selecting only a subset of relay nodes brings better performances with respect to using all “good-nodes” as relays or using only a single relay node.

Dedicated-multichannel-MAC (DMMAC) is an hybrid MAC protocol that uses both TDMA and CSMA/CA schemes.⁴¹ It exploits the adaptive-broadcasting mechanism for guaranteeing collision-free and delay-bounded transmission for safety applications.

3 | PROBLEM STATEMENT

This section identifies the critical issues in the considered IoV scenario and the factors for addressing them.

3.1 | Considered scenario

Electronics systems embedded in vehicles are constrained by definition, thus cloud platforms (remote servers) are needed to centralize data, analyze them, and then send back the user some useful information. More in detail, the heterogeneous nature of IoV makes it difficult to manage the data gathered due to the following issues.

- *Mobility support*. Since vehicles in an IoV scenario are always in motion, a delay on the remote, centralized computing frameworks may result too large for providing efficient services in mobility applications.⁴² Timeliness is indeed a fundamental requirement: the system needs to be able to provide the information in time and to determine how to handle an event at a certain instant. Transmitting data at the exact time and in the exact place is critical as vehicles are in motion.
- *Latency*. The real-time availability of data is a key requirement of IoV, strictly related to the mobility issue. The centralized cloud framework provides a series of services by collecting data and processing them. Any decision taken by the cloud framework has to travel to a specific location in the IoV system. Transmission of these decisions may take some time to get to the desired destination, depending on the configuration of the channels and actors transmitting the information. Thus, the latency between the packet sending and its reception has to be considered. This means defining a QoS model to analyze the traffic flow depending on the requirements of the packet transmission.

- *Scalability.* Several technologies are exploited to create communication between smart devices, mobile networks, and roadside IoT, to implement the IoV. The heterogeneity of IoV must be properly supported.
- *Energy efficiency.* Networks and cloud data centers are stressed due to the high number of devices interconnected in the IoV, producing and transmitting data. This huge workload makes it necessary to ensure the efficient management and transmission of the data, without compromising the energy efficiency of employed devices. A single node which drained its battery creates inefficiency in the whole network.

The considered scenario is depicted in Figure 1. Data are collected via diverse ITS applications and transmitted through bridge nodes. They then arrive to the sink node (a centralized cloud computing device) to be stored and exploited for the smart city tasks (e.g., dynamic synchronization of traffic lights, intelligent illumination of urban and extra-urban roads, traffic

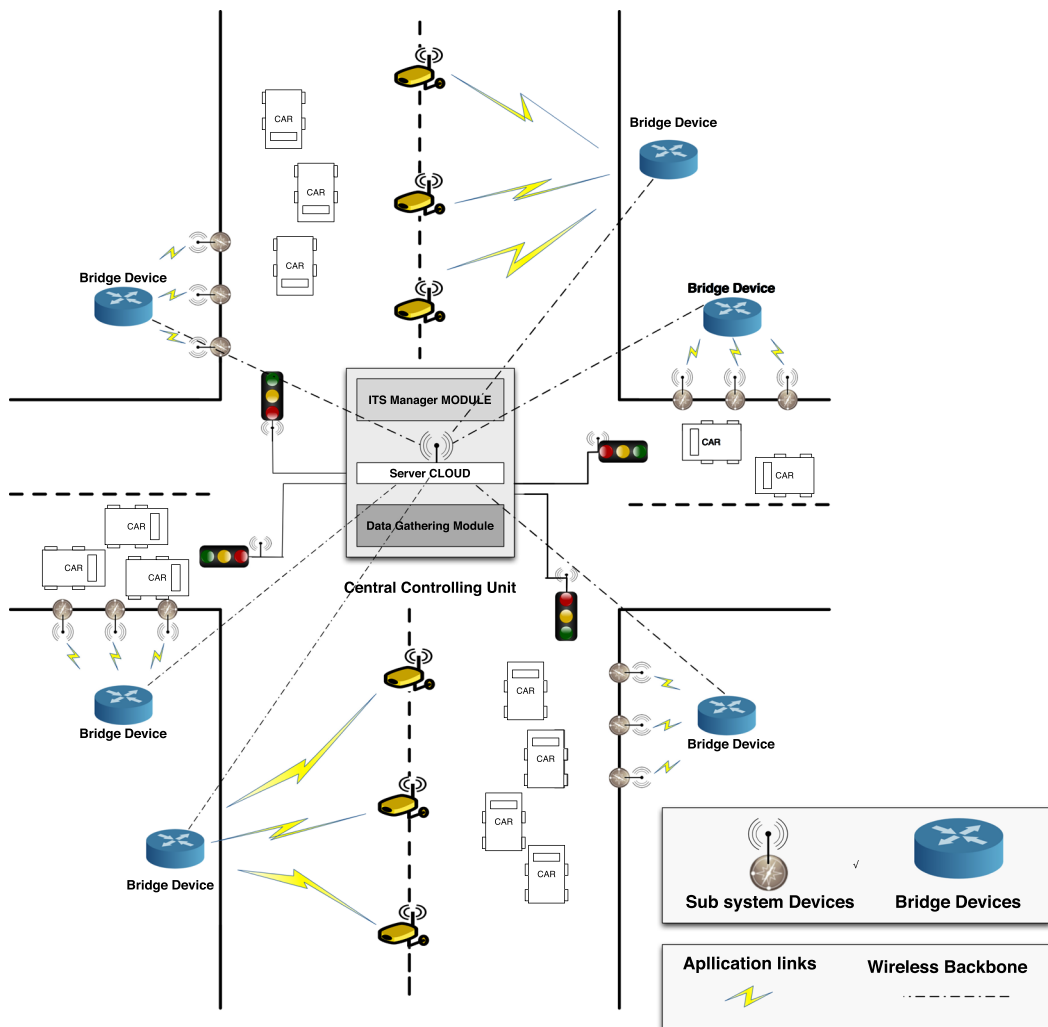


FIGURE 1 Architecture of the considered Internet of vehicles (IoV) scenario [Color figure can be viewed at wileyonlinelibrary.com]

jam vehicle-to-vehicle communications, and so on). However, bridge nodes are usually battery-powered devices that cannot be permanently powered on to guarantee low latency and high QoS. Therefore a trade-off approach is required.

3.2 | Goals

Two factors are considered to address the critical issues listed in Section 3.1:

- *Energy efficiency* should be maximized, as the smart energy grid would benefit from the reduction in the operational power and maintenance costs. In particular, the solution proposed in this paper aims at improving the energy efficiency for IoV bridge nodes, which transmit most of the information.
- *QoS* should be achieved without sacrificing the limited charge available on the device. According to the context described in Section 3.1, the concept of QoS comprises many facets: the *timeliness* of the transmission of the data, the ability of sending data to the control logic and then back on the field where it is needed; the *latency* which has to be kept low enough for effective timeliness, but not too low to avoid excessive power consumption; the *scalability*, which is the possibility to apply this kind of management system to an ever growing number of smart city applications, with data hopping through a network bridge after the other.

4 | PROPOSED APPROACH

IEEE 802.11 standard is commonly used for local and Internet connection, and widely used for IoT devices in home and industry settings. Thanks to its flexibility, several IEEE 802.11 amendments have been proposed for different industrial applications. Table 1 shows the characteristics of different IEEE 802.11 standards.^{43,44} The IEEE 802.11p amendment was born to facilitate vehicle to vehicle communication. With respect to other IEEE 802.11 standards, it offers a good trade-off between speed and range. In fact, IEEE 802.11p enables the largest communication distance, since it is based on an OFDM (orthogonal frequency division multiplexing) physical layer. The OFDM removes inter symbol interference (ISI) and improves signal to noise ratio (SNR) to have good communication quality over long distances.^{45–48}

TABLE 1 IEEE 802.11 standards type

Type	PHY	Frequency (GHz)	Bandwidth (MHz)	Speed (Mbit/s)	Range outdoor (m)
802.11	DSSS/FHSS	2.4	22	2	100
802.11b	HR-DSSS	2.4	22	11	140
802.11a	OFDM	5	5/10/20	54	120
802.11p	OFDM	5.9	5/10/20	54	1000
802.11n	HT-OFDM	2.4/5	20/40	288/600	250
802.11ax	HE-OFDM	2.4/5/6	20/40/80/80+80	1147 to 9608	120
802.11ac	VHT-OFDM	5	20/40/80/160	346 to 3466	NA

Nevertheless, IEEE 802.11p still has high power consumption requirements to cover such long distances.^{49,50} This paper addresses this issue of IEEE 802.11p, by proposing a novel technique to dramatically decrease its power consumption.

IEEE 802.11p introduces the possibility for two vehicles to establish a temporary point-to-point communication thanks to *WAVE Mode*. In *WAVE mode* a station can send and receive frames using a wildcard basic service set (BSS) ID, removing the need for the BSS joining procedure. This mechanism becomes useful for delay-critical frames, where the time needed for joining to a BSS may bring critical consequence on the time needed for the frame reception. However, the extensive usage of this mode can cause a high increase in the number of collisions, thus it has to be kept only for safety-critical situations. For other less delay-constrained scenarios, IEEE 802.11p introduces another type of service set, called WAVE basic-service-set (WBSS): this is the set of stations anchored to the owner access-point (AP). As for classic IEEE 802.11 BSS, in IEEE 802.11p AP devices play the role of coordinators of their own WBSS and each of them sends periodically an advertise message containing information about the services offered and the parameters of its own WBSS. In this way, receiver stations can decide whether to join, and eventually they already know the configuration procedure for becoming member of the service set.⁵¹

The approach proposed in this paper is designed to fit nodes of a multi-tiered architecture with controlling capabilities on end devices, and therefore the work is solely focused on the WBSS-related part of the IEEE 802.11p standard. Figure 1 shows an example of a multi-tiered network. Here, the central controlling unit (CCU), which is a central, remote, and unconstrained device, computes the duty cycle (i.e., active/sleeping time) and transmission power for bridge devices. The proposed approach greatly benefits QoS, by ensuring timeliness data transfer for all necessary data transmissions, and by monitoring traffic flow on the network and duty cycle of end devices.

As shown in Figure 2, the proposed solution manages operational duty cycle and transmission power to minimize the battery consumption of the bridge device, to extend its battery life. Two FLCs are used: FLC_1 governs operational duty cycle of a device as described in Section 4.1; FLC_2 governs transmission power, as described in Section 4.2. The FLCs are assumed to be embedded within APs, which are charged to compute active/sleeping times and to communicate their changes to the target device. In this way, since computation is performed locally, no further messages with the devices are required. Moreover, the sleeping time of the stations is constant and pre-determined, so the AP can easily know it.

4.1 | Sleeping time management

When end nodes are in active state, the network bridge receives periodic messages as soon as they sample data. Instead, when end nodes enter in sleeping mode, they keep on sampling data, but without transmitting them. These data are then transmitted to the bridge node as soon as the end node switches back to active state. It should be noted that, since end nodes can have different sleeping time, the bridge device could receive messages from end devices at different time intervals. This is not an issue, since bridge devices are always active, as they are connected to the power grid.

FLC_1 computes the active duty cycle time for a device, given its *battery level* and *throughput to workload ratio*: Th/Wl . *Throughput* is defined as the total number of packets sent in a time

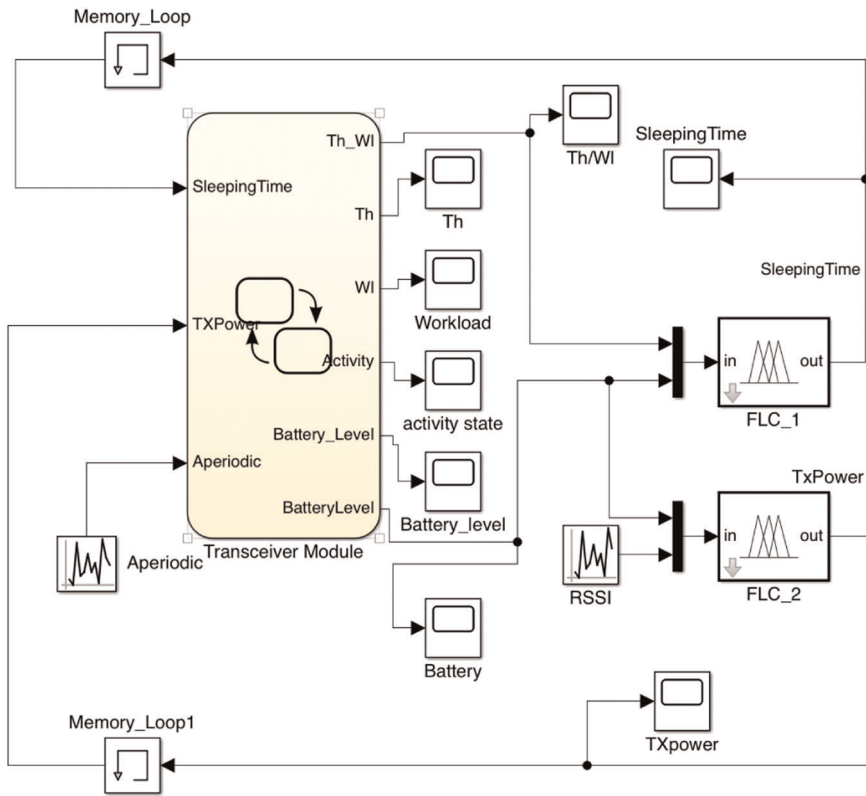


FIGURE 2 Simulink scheme for the simulation of the proposed approach [Color figure can be viewed at wileyonlinelibrary.com]

unit by the device and effectively reaching destination. *Workload* is defined as the number of packets that the device should send in a time unit.

Traffic flow can be usually split into two categories: *periodic* and *aperiodic*. The former is made of data which are sampled and transmitted by end devices at specific time intervals; the latter is made of data transmitted in case of an unforeseeable event happens (e.g., in a car accident). In periodic traffic, the time interval between two consecutive transmissions could be different, depending on the real quantity to sample. An interval time T_{LCM} can be considered for each device, computed as the least common multiple (LCM) of all its periodic packets. Thus, at each T_{LCM} a device should send $TotPP$ periodic packets:

$$TotPP = \sum_{t=T_{start}}^{T_{stop}} \Psi(t), \quad (1)$$

where T_{start} and T_{stop} represent time instants bounding T_{LCM} , and $\Psi(t)$ is an indicator function thus defined:

$$\Psi(t) = \begin{cases} 0 & t \bmod T_s \neq 0 \\ 1 & t \bmod T_s = 0 \end{cases} \quad (2)$$

with T_s being the device sampling time.

Aperiodic packets are instead messages which are rarely transmitted. They are either transmitted just once (e.g., alarm-like messages), or they may be generated and sent on an event-driven base (e.g., traffic jam notification due to a car accident). However, in the latter case a new message is transmitted only after a certain threshold time. It is not possible to predict the distribution of aperiodic packets on a certain time window T_{LCM} . However, it is theoretically possible to gauge their total number, $TotAP$, depending on the aperiodic traffic forecasted over the network.

The throughput to workload ratio (Th/Wl) can be calculated as

$$Th/Wl = \frac{k + TotAP}{TotPP + TotAP}. \quad (3)$$

All aperiodic packets received by the end device while sleeping are transmitted to the network controller, while only k periodic packets can be transmitted. A selection strategy is required to select the packets to send at the periodic time interval. For example, only the n most recent packets can be taken, or packets can be taken at regular time intervals (so increasing the sampling time). Sending fewer packets has upsides: the awake time could be not enough to transmit all the packets collected during the sleep time; however, the possibility of packet collision with other devices is reduced due to the lower traffic.

The crisp parameter ranges for FLC_1 are:

- Th/Wl : $[0, 100]$ in percentage.
- battery level: $[0, 100]$ in percentage.
- sleeping time: $[0, 10] \cdot BI \cdot T_s$, in seconds. BI is the *beacon interval* in IEEE 802.11. T_s is the constant *sampling time* set at design time for each device.

Three *membership functions* (*High*, *Medium*, *Low*) are defined for each parameter, to map its crisp value to a 0/1 membership value. Then, some inference rules with several IF-THEN-ELSE statements are defined, to state the output of membership functions. Finally, a crisp output is mapped to the x coordinate of the shape center of gravity:

$$sleepT = \frac{\sum_{i=1}^n Out_i \times C_i}{\sum_{i=1}^n C_i}, \quad (4)$$

where C_i is the center of the i th output membership function and Out_i is the output of the i th rule.

4.2 | Transmission power management

The second fuzzy logic controller FLC_2 computes the transmitting power of each end device in its active state, depending on the battery level and the actual RSSI value. The crisp values of the I/O parameters are:

- battery level: $[0, 100]$ in percentage.
- RSSI: $[0, 255]$, where 0 is the worst value and 255 is best link quality.
- transmission power: $[0, 100]$ in percentage, highest transmission power being 100%.

The output of FLC_2 is computed in the same way as for FLC_1 . Transmission power is defuzzified with the centroid mechanism, as in (4).

4.3 | System model

Figure 2 depicts the Matlab/Simulink model built to simulate the proposed approach. *Sleeping time* and *Transmission power* are the two inputs of *Transceiver Module* block in a feedback loop system. The *Aperiodic* input is the total number of aperiodic packets to be transmitted when the node is active. This parameter takes values in the interval 0–5, the majority of the packets being made of periodic packets.

The outputs are Th/Wl and the battery level. The battery level is managed as a finite state machine inside Simulink/Stateflow. This finite state machine, as shown in Figure 3, states the power consumption of the device depending on its active/sleeping state.

5 | SIMULATED SCENARIO

This section describes the simulated scenario. The parameters for the simulation are taken from the data-sheets of the simulated components:

- RN171 2.4 GHz IEEE Standard 802.11 b/g Wireless LAN Module;⁵²
- VERAP-173 chipset based on IEEE Standard 802.11p Wireless Module;⁵³
- 16 bit micro-controller - Microchip PIC24F family (PIC24FJ256GB108).⁵⁴

The simulated battery is a 10.8 V lithium-ion battery. Its full capacity is $fullBattery = 3100\text{mAh}$, which corresponds to $maxBit = 1023$ bits, using a 10-bit analog-to-digital converter.

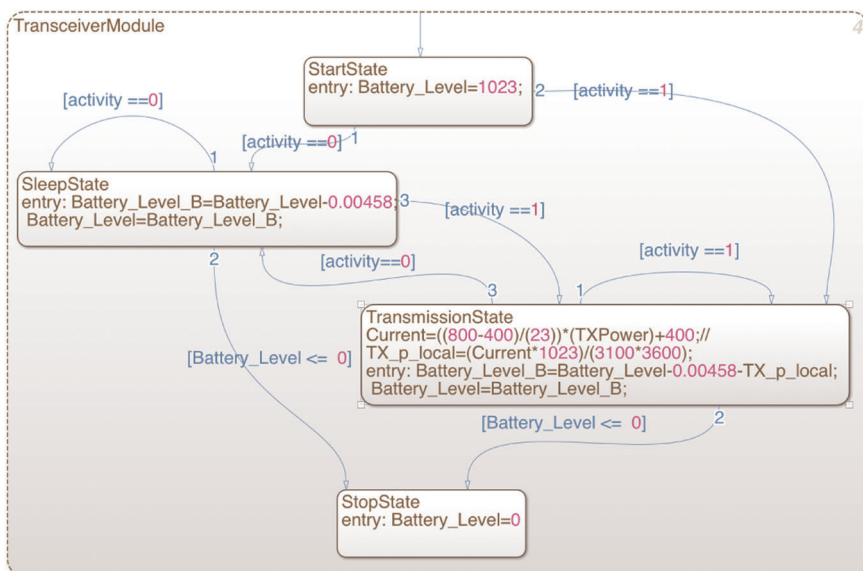


FIGURE 3 Finite state machine of the battery level [Color figure can be viewed at wileyonlinelibrary.com]

The parallel FLCs take in input the RSSI values and the outputs of *Transceiver Module* (Figure 2). RSSI spans random values in a certain range (the limits are obtained via experimental measures).

The total power consumed by the device is due to:

- $P_{\mu C} = 50 \text{ mAh}$ for data acquisition and elaboration performed by the PIC24F microcontroller;
- $P_{RF} = 240 \text{ mAh}$ for transmission power $T \times P = [0, 12] \text{ dBm}$, due to the IEEE 802.11 module consumption.
- $P_{RF} = 800 \text{ mAh}$ for transmission power $T \times P = [0, 23] \text{ dBm}$, due to the IEEE 802.11p module consumption.

The amount of P_{RF} depends on the active/sleeping state of the device. In sleep mode, the power is almost due to the microcontroller alone, since $P_{RF \text{ sleep}} = 4 \mu\text{Ah}$. This value can be converted into a digital value using the 10-bit AD converter with this proportion:

$$P_{\mu C}: \text{fullBattery} = D_{\text{sleep}(1\text{hour})}: \text{maxBit}, \quad (5)$$

where D_{sleep} is the digital value of the power consumption per time unit in sleep mode. D_{sleep} can be derived in this way:

$$D_{\text{sleep}} = \frac{P_{\mu C} \times \text{maxBit}}{\text{fullBattery} \times 3600} = 0.00458 \text{ bit/s}. \quad (6)$$

Since 1 h is made of 3600 s. This means that every second, the digital value of the battery charge decreases of 0.00458 bit/s.

While the device is instead in active mode, its power consumption is surely higher:

$$D_{\text{transmit}} = D_{\text{sleep}} + \frac{P_{RF \text{ transmit}} \times \text{maxBit}}{\text{fullBattery} \times 3600}. \quad (7)$$

In this formula, $P_{RF \text{ transmit}}$ refers to the transmission power. In IEEE 802.11 Wireless LAN case, P_{RF} goes from 240 mAh⁵² at highest possible transmission power (12 dBm) to 135 mAh at lowest transmission power (0 dBm). In IEEE 802.11p case, P_{RF} goes from 800 mAh at 23 dBm to 400 mAh at 0 dBm. Values between maximum and minimum are calculated through interpolation inside *Transceiver Module* in Figure 2. These values are listed in Tables 2 and 3.

TABLE 2 Interpolation of the power consumption for IEEE 802.11

Transmission power (dBm)	$P_{RF \text{ transmit}}$ (mAh)	D_{transmit} (bit/s)
0	135	0.01696
2	152.5	0.01856
4	170	0.02017
6	187.5	0.02177
8	205	0.02338
10	222.5	0.02498
12	240	0.02658

TABLE 3 Interpolation of the power consumption for IEEE 802.11p

Transmission power (dBm)	$P_{RF\ transmit}$ (mAh)	$D_{transmit}$ (bit/s)
0	400	0.0367
2	343.7	0.0315
4	469.5	0.0430
6	504.3	0.0462
8	539.1	0.0494
10	573.9	0.0526
12	608.6	0.0558
14	643.4	0.0590
16	678.2	0.0622
18	713.038	0.0654
20	747.820	0.0686
23	800	0.0733

6 | FLC DESIGN THROUGH EXPERIMENTAL RESULTS

The design process of FLC_1 and FLC_2 has been organized in a series of steps. First, FLC_1 was tested alone, with the ensemble of rules listed in Table 4. These rules aim at obtaining an acceptable compromise between QoS parameters and power consumption. Three main shapes of membership functions have been applied to the Fuzzy algorithm: Gaussian, Triangular and Trapezoidal. The combinations of these three functions are listed in Table 5. Each membership combination has been applied to the model of FLC_1 fuzzy block and then simulated in Matlab. Simulation results are reported as battery lifetime for each combination in Table 5. The configuration of membership functions for FLC_1 achieving the highest battery life is **Triangular-Triangular-Gaussian**, highlighted in bold in the table.

TABLE 4 Set A of inference rules for FLC_1

Rule	Antecedent (Th/Wl)	Antecedent (battery level)	Consequent (sleeping time)
1	Low	Low	Medium
2	Low	Medium	Low
3	Low	High	Low
4	Medium	Low	Medium
5	Medium	Medium	Medium
6	Medium	High	Low
7	High	Low	High
8	High	Medium	High
9	High	High	High

TABLE 5 Battery life of a station according to the shape of the membership functions of FLC_1

Antecedent (Th/Wl)	Antecedent (battery level)	Consequent (sleeping time)	Battery life (s)
Triangular	Triangular	Triangular	79,712
Triangular	Triangular	Trapezoidal	78,924
Triangular	Triangular	Gaussian	79,912
Triangular	Trapezoidal	Triangular	79,522
Triangular	Trapezoidal	Trapezoidal	79,224
Triangular	Trapezoidal	Gaussian	79,424
Triangular	Gaussian	Triangular	79,423
Triangular	Gaussian	Trapezoidal	79,030
Triangular	Gaussian	Gaussian	79,432
Trapezoidal	Triangular	Triangular	79,851
Trapezoidal	Triangular	Trapezoidal	79,424
Trapezoidal	Triangular	Gaussian	79,617
Trapezoidal	Trapezoidal	Triangular	79,636
Trapezoidal	Trapezoidal	Trapezoidal	79,347
Trapezoidal	Trapezoidal	Gaussian	79,123
Trapezoidal	Gaussian	Triangular	79,119
Trapezoidal	Gaussian	Trapezoidal	78,653
Trapezoidal	Gaussian	Gaussian	79,152
Gaussian	Triangular	Triangular	79,622
Gaussian	Triangular	Trapezoidal	79,233
Gaussian	Triangular	Gaussian	79,638
Gaussian	Trapezoidal	Triangular	79,465
Gaussian	Trapezoidal	Trapezoidal	79,073
Gaussian	Trapezoidal	Gaussian	79,234
Gaussian	Gaussian	Triangular	79,332
Gaussian	Gaussian	Trapezoidal	78,953
Gaussian	Gaussian	Gaussian	79,279

Next, different fuzzy rules are checked to tune the Th/Wl ratio. The following set of rules for FLC_1 were compared to esteem their different impact:

- A** rules shown in Table 4;
- B** rules in Table 4 are modified by taking into account only Th/Wl . The sleeping time behaves in the same way (high \rightarrow high/low \rightarrow low) as Th/Wl .

- C only battery level is considered in the rules in Table 4. The sleeping time behaves in the opposite way with respect to the battery level (high → low/low → high).
- D the sleeping time is computed as an algebraic combination of the input parameters.

For what concerns *Th/Wl*:

$$value = \begin{cases} 1 & \text{if } Th/Wl \text{ high} \\ 0 & \text{if } Th/Wl \text{ medium} \\ -1 & \text{if } Th/Wl \text{ low} \end{cases}$$

Instead, for what concerns battery level:

$$value = \begin{cases} 1 & \text{if } batteryLevel \text{ low} \\ 0 & \text{if } batteryLevel \text{ medium} \\ -1 & \text{if } batteryLevel \text{ high} \end{cases}$$

Sleeping time is then calculated as the algebraic sum of these values.

$$sleepTime = \begin{cases} Low & \text{if } sum < 0 \\ Medium & \text{if } sum = 0 \\ High & \text{if } sum > 0 \end{cases}$$

The only differences with respect to rules in Table 4 are for rules 4 (high instead of medium) and 9 (medium instead of high).

Table 6 reports the results obtained with different rules for *FLC*₁ by using the membership function shapes with the longest battery lifetime, that is, **Triangular-Triangular-Gaussian** as shown in Table 5. Finally, the highest value of battery lifetime is achieved with set C, whereas set B gives the highest *Th/Wl* ratio.

The same approach was used to design *FLC*₂ when used in conjunction with *FLC*₁. The set of rules used for *FLC*₁ and *FLC*₂ are listed in Tables 4 and 7, respectively. The combination of membership functions shapes for *FLC*₁ are Triangular-Triangular-Gaussian, as previously found, whereas different combinations for *FLC*₂ were tested to maximize the battery lifetime. The same shapes of membership functions are considered: Gaussian, Triangular, and Trapezoidal. The resulting values of battery life for each combination are reported in Table 8. The longest battery lifetime combination is **Gaussian-Trapezoidal-Gaussian**, highlighted as bold text in Table 8: the battery can operate for 80,092 s (around 22 h) with this combination.

Then, different set of rules for *FLC*₂ are checked to tune *Th/Wl*:

TABLE 6 Comparison among the sets of rules for *FLC*₁

	Battery life (s)	Th/Wl (%)
A	79,912	34.0
B	81,223	34.7
C	85,151	29.9
D	82,293	33.0

TABLE 7 Set A of inference rules for FLC_2

Rule	Antecedent (battery level)	Antecedent (RSSI)	Consequent (transmission power)
1	Low	Low	Medium
2	Low	Medium	Medium
3	Low	High	Low
4	Medium	Low	Medium
5	Medium	Medium	High
6	Medium	High	Low
7	High	Low	High
8	High	Medium	Medium
9	High	High	Low

A default rules as in Table 7;

B rules that assign to the transmission power the same behavior (high \rightarrow high/low \rightarrow low) as the battery level.

C rules taking into account only RSSI: the behavior of transmission power is the opposite (high \rightarrow low/low \rightarrow high).

D rules calculating transmission power as an algebraic combination of the input parameters.

For what concerns battery level:

$$value = \begin{cases} 1 & \text{if } batteryLevel \text{ high} \\ 0 & \text{if } batteryLevel \text{ medium} \\ -1 & \text{if } batteryLevel \text{ low} \end{cases}$$

Instead, for what concerns RSSI:

$$value = \begin{cases} 1 & \text{if } RSSI \text{ low} \\ 0 & \text{if } RSSI \text{ medium} \\ -1 & \text{if } RSSI \text{ high} \end{cases}$$

The transmission power is calculated as the sum of the two addends:

$$value = \begin{cases} Low & \text{if } sum < 0 \\ Medium & \text{if } sum = 0 \\ High & \text{if } sum > 0 \end{cases}$$

The differences of this set of rules with respect to those in Table 7 regarding rules 2 (low instead of medium), 4 (high instead of medium), 5 (medium instead of high) 8 (high instead of medium), and 9 (medium instead of low).

TABLE 8 Battery life of a station according to the shape of the membership functions of FLC₂

Antecedent (battery level)	Antecedent (RSSI)	Consequent (transmission power)	Battery life (s)
Triangular	Triangular	Triangular	79,912
Triangular	Triangular	Trapezoidal	79,711
Triangular	Triangular	Gaussian	79,964
Triangular	Trapezoidal	Triangular	79,942
Triangular	Trapezoidal	Trapezoidal	79,904
Triangular	Trapezoidal	Gaussian	80,046
Triangular	Gaussian	Triangular	79,722
Triangular	Gaussian	Trapezoidal	79,615
Triangular	Gaussian	Gaussian	79,798
Trapezoidal	Triangular	Triangular	79,821
Trapezoidal	Triangular	Trapezoidal	79,704
Trapezoidal	Triangular	Gaussian	79,858
Trapezoidal	Trapezoidal	Triangular	79,874
Trapezoidal	Trapezoidal	Trapezoidal	79,829
Trapezoidal	Trapezoidal	Gaussian	79,897
Trapezoidal	Gaussian	Triangular	79,711
Trapezoidal	Gaussian	Trapezoidal	79,659
Trapezoidal	Gaussian	Gaussian	79,754
Gaussian	Triangular	Triangular	79,858
Gaussian	Triangular	Trapezoidal	79,754
Gaussian	Triangular	Gaussian	79,904
Gaussian	Trapezoidal	Triangular	80,069
Gaussian	Trapezoidal	Trapezoidal	79,866
Gaussian	Trapezoidal	Gaussian	80,092
Gaussian	Gaussian	Triangular	79,730
Gaussian	Gaussian	Trapezoidal	79,570
Gaussian	Gaussian	Gaussian	79,747

The system was simulated for each set of rule, keeping the **Gaussian-Trapezoidal-Gaussian** membership function shapes for FLC₂. The results of the simulation for *Th/Wl* and battery lifetime are reported in Table 9. Despite the fact that *Th/Wl* does not influence the output of FLC₂, it is reported as an indicator of transmission performance in Table 9. As highlighted in the table, set B achieves the highest battery life, whereas set C achieves the highest *Th/Wl*.

TABLE 9 Comparison among the sets of rules for FLC₂

	Battery life (s)	Th/Wl (%)
A	80,092	33.86
B	80,714	33.72
C	80,145	34.08
D	80,546	33.75

A final round of simulation considered both the FLCs, aiming to identify the best combination of rules for both of them. Table 10 reports the results for all possible permutations of set of rules. Among them, the one achieving the highest battery life is CB, highlighted in bold text. This confirms the partial results obtained in Table 6 and Table 9. This configuration keeps *Th/Wl* around 34%. The CB configuration is thus the one chosen for the evaluation of the proposed approach in Section 7.

It goes without saying that the more energy is saved, the more the performance degrades. Tables 6, 9, and 10 clearly show a value of *Th/Wl* less than 40%. Despite this, please note that these values are averaged during the whole simulation: the lower the battery level, the fewer the packets transmitted. This may seem a limitation, but it is compliant with the aim of the FLCs. Instead, the reduced transmitted data has two upsides: the network traffic is reduced and so is the probability of collision; the transmitted data do not contain the same values due to oversampling. It is indeed possible to state that the FLCs are energy-efficient schedulers, since they adjust the amount of transmitted data depending on the battery level.

TABLE 10 Permutations of the sets of rules of the FLCs

	Battery life (s)	Th/Wl (%)
1-AA	80,092	33.86
2-AB	80,714	33.72
3-AC	80,145	34.08
4-AD	80,546	33.75
5-BA	81,452	34.75
6-BB	81,947	34.76
7-BC	81,431	34.77
8-BD	81,794	34.69
9-CA	85,438	29.95
10-CB	86,106	29.71
11-CC	85,418	30.10
12-CD	85,802	29.78
13-DA	82,563	32.99
14-DB	83,166	32.80
15-DC	82,618	33.10
16-DD	83,030	32.89

7 | SIMULATION RESULTS

The goal of this section is to evaluate the performance of the proposed algorithm so as to reach higher battery lifetime in a vehicular network application. The VERAP-173 IEEE 802.11p module is used to evaluate the network performance. The power transmission of this module is $P_{TX}=[0\ 23]$ dBm. When the module operates at maximum transmission power, it consumes 800 mAh. Simulink Matlab R2020a has been used to simulate system, and the model was implemented using the StateFlow block and Fuzzy logic toolbox in Simulink, as shown in Figure 2. The power consumption model is implemented from Equation (7) in the StateFlow block in the Simulink environment. The optimal fuzzy configuration has been used in a 45 h long simulation.

As Figure 4 shows, for the IEEE 802.11p protocol the battery lifetime is 44,914 s (about 12 h) when the device is set with the highest sampling rate and 0 s sleeping time. The Th/Wl is 99.99% in this configuration, since the system is continuously sending data at the highest throughput. If the sleeping time is increased to 3 s, the battery lifetime reaches 66,014 s (about 18 h), with a Th/Wl ratio of 41%. As expected, the battery lifetime increases by applying the proposed fuzzy logic solution for the IEEE 802.11p protocol, reaching 86,106 s (about 24 h).

In addition, simulation results when adopting IEEE 802.11 b/g, another wireless WiFi technology, are presented in Figure 5. Here, the battery lifetime reaches 100,574 s (about 27 h) and Th/Wl is 99% if the sleeping time is set to 0 s. Moreover, by setting the sleeping time to 3 s, the battery lifetime goes up to 128,923 (about 35 h) with Th/Wl about 41%; in both fixed sleeping time, the transmission power was set to 11.5 dBm. However, better results are obtained by means of the FLCs: the battery lifetime increases to 148,784 s (about 40 h) with Th/Wl about 31%.

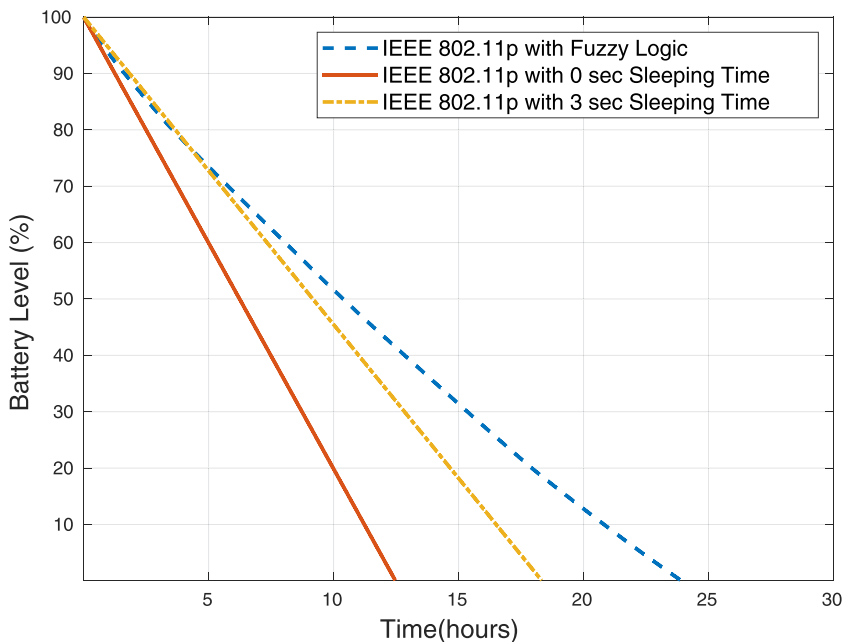


FIGURE 4 Battery consumption in IEEE 802.11p scenario [Color figure can be viewed at wileyonlinelibrary.com]

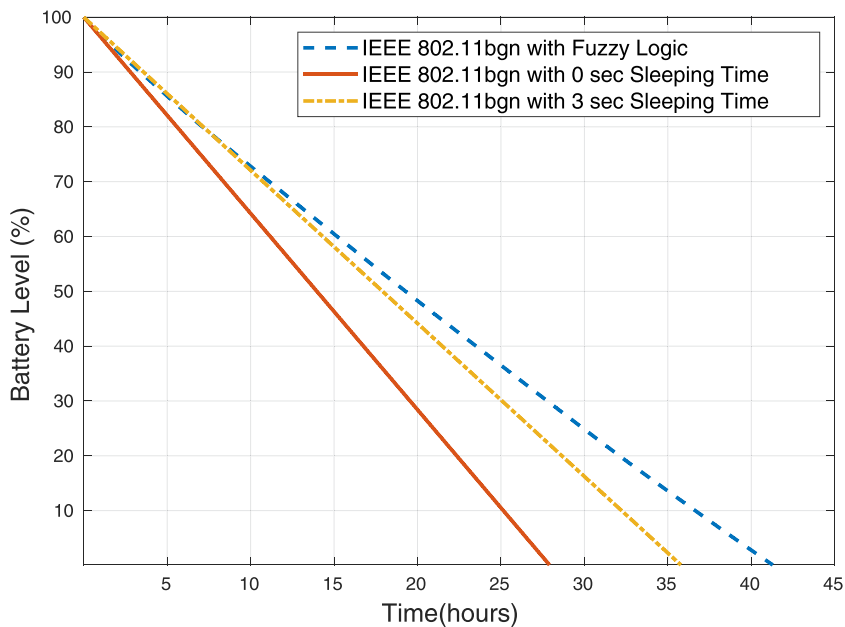


FIGURE 5 Battery consumption in IEEE 802.11b/g/n scenario [Color figure can be viewed at wileyonlinelibrary.com]

Table 11 summarizes the performance, in terms of battery lifetime and Th/Wl, of different configurations of the two considered Wi-Fi technologies. First of all, increasing the length of the sleeping time directly impacts on the energy consumption: the battery lifetime is prolonged because the node does not transmit data while sleeping. Avoiding the data transmission during sleeping reduces the workload. Its effect on throughput cannot be easily predicted: from one hand, few packets are transmitted, but on the other hand the packet congestion is less likely. Overall, as can be seen in Table 11, a longer sleeping time reduces Th/Wl. The proposed approach based on the two FLCs increases the battery lifetime dramatically, with a moderate Th/Wl loss. In detail, with the IEEE 802.11b/g/n, the FLCs increase the battery lifetime up to 47% with respect to the basic system with 0 s of sleeping time, and up to 15% with a sleeping time of 3 s. With the IEEE 802.11p technology, battery lifetime raises up to 91% with respect to the basic system with 0 s of sleeping time, and up to 30% with 3 s of sleeping time. In both cases with fixed sleeping time, the transmission power has been set to 11.5 dBm.

TABLE 11 Improvement of battery lifetime (%) with the fuzzy logic controllers

Technology	Battery life (s)			Th/Wl (%)		
	Original	With FLCs	Change	Original	With FLCs	Change
IEEE 802.11b/g/n, sleeping time 0 s	100,574	148,784	+48%	99.99	31.14	−31%
IEEE 802.11b/g/n, sleeping time 3 s	128,923	148,784	+15%	41.20	31.14	−24%
IEEE 802.11p, sleeping time 0 s	44,914	86,106	+92%	99.99	29.71	−70%
IEEE 802.11p, sleeping time 3 s	66,014	86,106	+30%	41.26	29.71	−28%

8 | CONCLUSION

This paper has proposed a methodology to increase energy efficiency and QoS in IOV networks. The approach aims to control the transmission power and duty cycle of a bridge device, that is, adjusting its sleeping time. In detail, two FLCs have been used to control the sleeping time and transmission power. The impact of the fuzzy controllers has been evaluated for two wireless technologies: IEEE 802p and IEEE 802.11b/n/g. A wide variety of combinations of membership functions have been evaluated for optimizing the performance of the controllers. The two controllers together are able to achieve the lowest power consumption, resulting in the longest battery life. Eventually, the battery life was around 24 h for IEEE 802.11p: the battery lifetime increases up to 91% with respect to a network where the sleeping time is fixed to 0 s and the transmission power is fixed to 11.5 dBm. The increase is up to 30% with respect to a network where the sleeping time is fixed to 3 s and the transmission power is fixed to 11.5 dBm. Moreover, the battery lifetime is about 40 h in IEEE 802.11b/g/n: the increase is 47% with respect to a fixed sleeping time of 0 s, and 15% when the sleeping time is fixed to 3 s, with the transmission power fixed to 11.5 dBm in both cases.

ACKNOWLEDGMENT

This study is in part supported by the Soonchunhyang University Research Fund.

ORCID

Mario Collotta  <https://orcid.org/0000-0003-0207-9966>

Renato Ferrero  <https://orcid.org/0000-0003-4459-4843>

Edoardo Giusto  <https://orcid.org/0000-0001-8371-6685>

Mohammad Ghazi Vakili  <https://orcid.org/0000-0002-2927-4975>

Jacopo Grecuccio  <https://orcid.org/0000-0002-6952-8490>

Xiangjie Kong  <https://orcid.org/0000-0001-9388-1879>

Il-sun You  <https://orcid.org/0000-0002-0604-3445>

REFERENCES

1. Li SE, Guo Q, Xu S, Duan J, Li S, Li C, et al. Performance enhanced predictive control for adaptive cruise control system considering road elevation information. *IEEE Trans Intell Veh.* 2017;2(3):150-160.
2. Stöckle C, Utschick W, Herrmann S, Dirndorfer T. Robust function and sensor design considering sensor measurement errors applied to automatic emergency braking. In: *IEEE Intelligent Vehicles Symposium*; 2019:2284-2290.
3. Song Y, Liao C. Analysis and review of state-of-the-art automatic parking assist system. In: *IEEE International Conference on Vehicular Electronics and Safety (ICVES)*, IEEE; 2016:1-6.
4. He YS, Guang XP, Tang ZY, He Y. Design and realization of vehicle navigation and monitoring system based on GPS and GIS. In: *2nd International Conference on Computer Science and Application Engineering*; 2018:1-6.
5. Sumalee A, Ho HW. Smarter and more connected: future intelligent transportation system. *IATSS Res.* 2018;42(2):67-71.
6. Altintas O, Dressler F, Hagenauer F, Matsumoto M, Sepulcre M, Sommery C. Making cars a main ICT resource in smart cities. In: *Conference on Computer Communications Workshops (INFOCOM)*, IEEE; 2015:582-587.
7. Qu F, Wu Z, Wang FY, Cho W. A security and privacy review of VANETs. *IEEE Trans Intell Transp Syst.* 2015;16(6):2985-2996.
8. Al Mallah R, Quintero A, Farooq B. Distributed classification of urban congestion using VANET. *IEEE Trans Intell Transp Syst.* 2017;18(9):2435-2442.

9. Zhu W, Gao D, Foh CH, Zhao W, Zhang H. A collision avoidance mechanism for emergency message broadcast in urban VANET. In: 2016 IEEE 83rd Vehicular Technology Conference (VTC Spring) IEEE; 2016:1-5.
10. Doolan R, Muntean GM. EcoTrec—A novel VANET-based approach to reducing vehicle emissions. *IEEE Trans Intell Transp Syst.* 2016;18(3):608-620.
11. Kaiwartya O, Abdullah AH, Cao Y, Altameem A, Prasad M, Lin CT, et al. Internet of vehicles: motivation, layered architecture, network model, challenges, and future aspects. *IEEE Access.* 2016;4: 5356-5373.
12. Contreras-Castillo J, Zeadally S, Guerrero-Ibañez JA. Internet of vehicles: architecture, protocols, and security. *IEEE Internet Things J.* 2017;5(5):3701-3709.
13. Gerla M, Lee EK, Pau G, Lee U. Internet of vehicles: from intelligent grid to autonomous cars and vehicular clouds. In: 2014 IEEE World Forum on Internet of Things, WF-IoT 2014; 2014.
14. Gerla M, Wu C, Pau G, Zhu X. Content distribution in VANETs. *Veh Commun.* 2014;1(1):3-12.
15. Atzori L, Floris A, Girau R, Nitti M, Pau G. Towards the implementation of the Social Internet of Vehicles. *Comput Netw.* 2018;147:132-145.
16. Li J, Zhang Y, Chen Y. A self-adaptive traffic light control system based on speed of vehicles. In: IEEE International Conference on Software Quality, Reliability and Security Companion (QRS-C) IEEE; 2016:382-388.
17. Chen C, Liu X, Qiu T, Liu L, Sangaiah AK. Latency estimation based on traffic density for video streaming in the internet of vehicles. *Comput Commun.* 2017;111:176-186.
18. Su KY, Mo YC, Chen LB, et al. An in-vehicle infotainment platform for integrating heterogeneous networks interconnection. In: IEEE International Conference on Consumer Electronics-Taiwan (ICCE-TW) IEEE. 2018:1-2.
19. IEEE. IEEE Standard for Information technology—local and metropolitan area networks—Specific requirements—Part 11: Wireless LAN Medium Access Control (MAC) and Physical Layer (PHY) Specifications Amendment 6: Wireless Access in Vehicular Environments. IEEE Std 80211p-2010 2010:1-51.
20. US Department of Transportation, National Highway Traffic Safety Administration. Vehicle Safety Communications Project—Final Report. DOT HS 810 591 2006 Apr:1-1291.
21. European Telecommunications Standards Institute. Intelligent Transport Systems (ITS); ITS-G5 Access layer specification for Intelligent Transport Systems operating in the 5 GHz frequency band. ETSI TS 102 687 V111 2019 May:1-24.
22. Association of Radio Industries and Businesses. 700 MHz Band Intelligent Transport Systems. ARIB STD-T109 Version 13 2017 Jul:1-245.
23. Pagliari DJ, Poncino M, Macii E. Energy-efficient digital processing via approximate computing. In: Smart Systems Integration and Simulation. Springer; 2016:55-89.
24. Chen Y, JahierPagliari D, Macii E, Poncino M. Battery-aware design exploration of scheduling policies for multi-sensor devices. In: Proceedings of the 2018 on Great Lakes Symposium on VLSI; 2018:201-206.
25. Darko AP, Liang D. An extended COPRAS method for multiattribute group decision making based on dual hesitant fuzzy Maclaurin symmetric mean. *Int J Intell Syst.* 2020;35(6):1021-1068.
26. Peng X, Krishankumar R, Ravichandran KS. Generalized orthopair fuzzy weighted distance-based approximation (WDBA) algorithm in emergency decision-making. *Int J Intell Syst.* 2019;34(10): 2364-2402.
27. Gao J, Xu Z. Differential calculus of interval-valued q-rung orthopair fuzzy functions and their applications. *Int J Intell Syst.* 2019;34(12):3190-3219.
28. Muneeza, Abdullah S, Aslam M. New multicriteria group decision support systems for small hydropower plant locations selection based on intuitionistic cubic fuzzy aggregation information. *Int J Intell Syst.* 2020; 35(6):983-1020.
29. Rahman MS, Manna AK, Shaikh AA, Bhunia AK. An application of interval differential equation on a production inventory model with interval-valued demand via center-radius optimization technique and particle swarm optimization. *Int J Intell Syst.* 2020;35(8):1280-1326.

30. Gillani SA, Shah PA, Qayyum A, Hasbullah HB. MAC layer challenges and proposed protocols for vehicular ad-hoc networks. *Adv Intell Syst Comput*. 2015;306:3-13.
31. Van Eenennaam EM, Karagiannis G, Heijenk GJ. Towards scalable beaconing in VANETs. Fourth ERCIM Workshop on eMobility; 2010:103-108.
32. Schmidt R, Leinmuller T, Schoch E, Kargl F, Schafer G. Exploration of adaptive beaconing for efficient intervehicle safety communication. *IEEE Netw*. 2010;24(1):14-19.
33. Patel A, Kaushik P. Improving QoS of VANET using adaptive CCA range and transmission range both for intelligent transportation system. *Wireless Pers Commun*. 2018;100(3):1063-1098.
34. Nguyen VD, Oo TZ, Tran NH, Hong CS. An efficient and fast broadcast frame adjustment algorithm in VANET. *IEEE Commun Lett*. 2017;21(7):1589-1592.
35. UshaRani B, Tarannum S. AMAC scheduling: to optimize QOS for DSRC. In: 2016 IEEE International Conference on Recent Trends in Electronics, Information and Communication Technology, RTEICT 2016—Proceedings; 2017:1543-1549.
36. Lim JMY, Chang YC, Loo J, Alias MY. Improving VANET performance with heuristic and adaptive fuzzy logic scheme. *Wireless Pers Commun*. 2015;83(3):1779-1800.
37. Patel A, Kaushik P. Improve QoS of IEEE 802.11p using average connected coverage and adaptive transmission power scheme for VANET applications. *Wireless Pers Commun*. 2017;95(4):3829-3855.
38. Omar HA, Zhuang W, Li L. Protocol for reliable broadcast in VANETs. *IEEE Trans Mobile Comput*. 2013;12(9):1724-1736.
39. Lim JH. Understanding STDMA via computer simulation: feasibility to vehicular safety applications, configurations, and time synchronization errors. *Eurasip J Wirel Commun Netw*. 2016;2016(1):1-14.
40. Zhang J, Zhang Q, Jia W. VC-MAC: a cooperative MAC protocol in vehicular networks. *IEEE Trans Veh Technol*. 2009;58(3):1561-1571.
41. Lu N, Ji Y, Liu F, Wang X. A dedicated multi-channel MAC protocol design for VANET with adaptive broadcasting. In: IEEE Wireless Communications and Networking Conference, WCNC No. May, IEEE; 2010:1-6.
42. Fernando N, Loke SW, Rahayu W. Mobile cloud computing: a survey. *Future Gener Comput Syst*. 2013;29(1):84-106.
43. Bellalta B, Bononi L, Bruno R, Kassler A. Next generation IEEE 802.11 Wireless Local Area Networks: current status, future directions and open challenges. *Comput Commun*. 2016;75:1-25.
44. Tramarin F, Vitturi S, Luvisotto M, Zanella A. On the use of IEEE 802.11n for industrial communications. *IEEE Trans Ind Inform*. 2016;12(5):1877-1886.
45. Almeida TT, de Carvalho Gomes L, Ortiz FM, Júnior JGR, Costa LHMK. IEEE 802.11p performance evaluation: simulations vs. real experiments. In: 2018 21st International Conference on Intelligent Transportation Systems (ITSC); 2018:3840-3845.
46. Arena F, Pau G, Severino A. A review on IEEE 802.11p for intelligent transportation systems. *J Sens Actuator Netw*. 2020;9(2):22.
47. Paier A, Faetani D, Mecklenbräuker CF. Performance evaluation of IEEE 802.11p physical layer infrastructure-to-vehicle real-world measurements. In: 2010 3rd International Symposium on Applied Sciences in Biomedical and Communication Technologies (ISABEL 2010); 2010:1-5.
48. Abdelgader AM, Lenan W. The physical layer of the IEEE 802.11 p WAVE communication standard: the specifications and challenges. In: Proceedings of the World Congress on Engineering and Computer Science; 2014;2:22-24.
49. Lin F, Liu Y. An integration of WAVE and LTE wireless transmission in vehicle networks for safety and non-safety messages dissemination. In: 2017 3rd IEEE International Conference on Computer and Communications (ICCC); 2017:315-320.
50. Chen S, Nai W, Dong D, Zheng W, Jing W. Key indices analysis of IEEE 802.11p based vehicle to infrastructure system in highway environment. *Proc Soc Behav Sci*. 2013;96:188-195. Intelligent and Integrated Sustainable Multimodal Transportation Systems Proceedings from the 13th COTA International Conference of Transportation Professionals (CICTP2013).
51. Jiang D, Delgrossi L. IEEE 802.11p: towards an international standard for wireless access in vehicular environments. In: IEEE Vehicular Technology Conference; 2008:2036-2040.

52. Microchip. RN171 Features; 2016. <https://www.microchip.com/wwwproducts/en/RN171>. Accessed December 31, 2020.
53. U-Blox. VERA-P1 series | u-blox. <https://www.u-blox.com/en/product/vera-p1-series>. Accessed December 31, 2020.
54. Microchip. PIC24FJ256DA210 Family Data Sheet 16-Bit Flash Microcontrollers with Graphics Controller and 2010. <https://www.microchip.com/wwwproducts/en/PIC24FJ256GB110>. Accessed December 31, 2020.

How to cite this article: Collotta M, Ferrero R, Giusto E, et al. A fuzzy control system for energy-efficient wireless devices in the Internet of vehicles. *Int J Intell Syst.* 2021;36: 1595–1618. <https://doi.org/10.1002/int.22353>